Design of a Compact Wideband Filtering Power Divider with Improved Isolation

Yijing Deng [1], Yixuan He [2], and Jianpeng Wang [1]

[1] Nanjing University of Science and Technology, Nanjing 210094, China
lillian-deng.y.j@outlook.com, eejpwang@gmail.com

[2] School of Information and Electronics
Beijing Institute of Technology, China
xuandd1995@126.com

Abstract ─ A novel design of wideband filtering power divider (FPD) with high selectivity, good isolation and widen upper stopband is presented in this paper. A new topology is proposed by adding an isolation resistor between two tri-mode resonators to guarantee the isolation. Besides, owing to the intrinsic characteristics of tri-mode resonators and coupled lines with one of them terminated by an open-circuited stub, four transmission zeros (*TZ*s) can be generated outside the operating band to improve the signal selectivity. For demonstration, a FPD operating at 2.35 GHz with 3-dB fractional bandwidth of 25.6% is designed, fabricated and measured. The measured isolation is better than 15.5 dB and the upper stopband is extended to 7.6 GHz ($3.23f_0$) with a rejection level of 20 dB.

Index Terms ─ Filtering power divider, synthesis design, tri-mode resonator, wide bandwidth.

I. INTRODUCTION

Nowadays, power dividers (PDs) and bandpass filters (BPFs) are frequently used in various microwave and millimeter-wave systems for power splitting/ combining and signal selection. These two components typically occupy an excessive area apiece, especially at low gigahertz frequency region. In order to obtain dual functions simultaneously with a relatively small area, it is beneficial to integrate the PD and BPF together.

Over the past few years, much effort has been focused on improving the performance of FPD based on compact size, high selectivity, good isolation, widen upper stopband, and etc. Embedded dual-mode resonator [1] and inductors with low impedance transmission lines [2] are introduced for compact size. Subsequently, short-circuited stub along with coupled lines [3] and open-ended transmission line [4] are utilized for high passband selectivity. Moreover, the isolation performance is a main consideration in FPD design. Isolation resistor added between two filters [5], net-type resonator [6] and distributed isolation network (DINW) [7] are proposed to provide improved isolation performance. Finally, widen upper stopband is achieved by replacing quarter-wavelength section with stepped impedance interdigital coupling element [8] and by creating TZ at the second harmonic frequency [9]. Although these studies presented satisfactory bandpass responses and power splitting properties, few of them have demonstrated wide stopband along with good isolation performance within the entire passband simultaneously.

The primary motivation of this paper is to design a wideband FPD with compact size, high selectivity, widen upper stopband and improved isolation. To achieve good isolation within not only the entire passband but also frequency region out of the operating band, a novel topology is proposed by adding an isolation resistor between the high-impedance stubs of two tri-mode resonators. Theoretical analysis is described to design the proposed FPD with prescribed performance. For demonstration, the proposed wideband FPD is designed, fabricated, and measured. Ultimately, both simulated and measured results validate the theoretical ones well.

II. CIRCUIT DESIGN OF THE PROPOSED FPD

Figure 1 shows the configuration of the proposed FPD. Owing to the intrinsic characteristic of tri-mode resonator and coupled lines with one of them terminated by an open-circuited stub, four transmission zeros (TZs) are generated to achieve high passband selectivity as well as deep stopband rejection. Besides, by adding an isolation resistor between high-impedance stubs of two tri-mode resonators, a novel topology is proposed for isolation improvement.

Submitted On: May 18, 2016
Accepted On: July 17, 2016

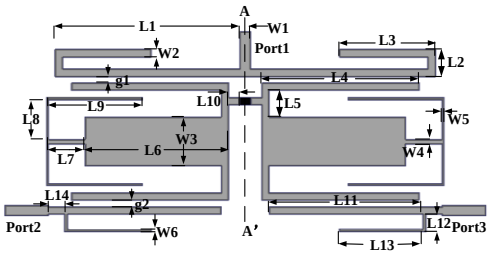

Fig. 1. Configuration of the proposed FPD.

A. Tri-mode resonator

When a signal is launched into the T-junction at Port 1, it will be equally split and delivered to the tri-mode resonators via coupling, thus engendering wideband filtering response as well as sharp roll-off skirt. The proposed tri-mode resonator shown in Fig. 2 (a) is symmetrical and can be analyzed by using odd- and even-mode methods. Under each resonance conditions, the input admittance can be derived as:

$$Y_{\text{int}rio} = Y_1 / (j \tan\theta_1) = 0, \tag{1}$$

$$Y_{\text{int}rie} = Y_1 \frac{Y_{\text{int}ri2} + jY_1 \tan\theta_1}{Y_1 + jY_{\text{int}ri2} \tan\theta_1} = 0, \tag{2}$$

where the input admittance Y_{intri2} of stepped-impedance resonator in Fig. 2 (c) yields:

$$Y_{\text{int}ri2} = jY_2 \frac{Y_2 \tan\theta_2 + Y_3 \tan\theta_3}{2Y_2 - 2Y_3 \tan\theta_2 \tan\theta_3}. \tag{3}$$

To simplify the analysis, here we set $\theta_1=\theta_2=\theta_3$, $2Y_3=Y_1$ and $M=Y_2/Y_3$, then the resonance conditions can be written as:

$$1/\ j\tan\theta_1 = 0, \tag{4}$$

$$M^2 + 5M - 4\tan^2\theta_1 = 0. \tag{5}$$

The first three resonant modes of the tri-mode resonator are expected as even-/odd-/even-modes with their resonant frequencies defined as f_o, f_{e1} and f_{e2} respectively. Specifically, with geometrical parameters listed in Table 1, the frequency response properties of the resonator are provided in Fig. 3. As shown in Fig. 3, two even-mode resonant frequencies can be observed at both sides of the odd-mode one under weak coupling situation ($g_1=g_2=0.5$ mm), while under strong coupling ($g_1=g_2=0.15$ mm), a wideband filtering response with a fractional bandwidth of 25.6% can be achieved, which verify the feasibility of proposed tri-mode resonator in wideband performance design.

Table 1: Dimension values of the proposed FPD (unit: mm)

W1	W2	W3	W4	W5	W6	L1	L2
1.11	0.5	7	0.2	0.1	0.1	22	2.5
L3	L4	L5	L6	L7	L8	L9	L10
15.6	15.7	2	19.8	4	4.5	8.8	0.9
L11	L12	L13	L14	g1	g2		
22	1.5	9.2	2	0.14	0.16		

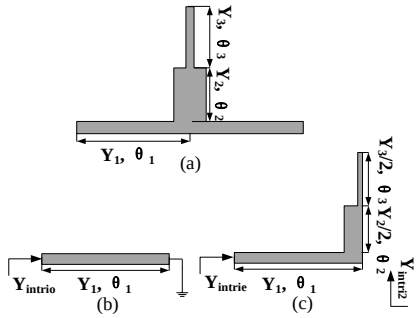

Fig. 2. Configuration of the proposed tri-mode resonator: (a) proposed tri-mode resonator, (b) odd-mode excitation, and (c) even-mode excitation.

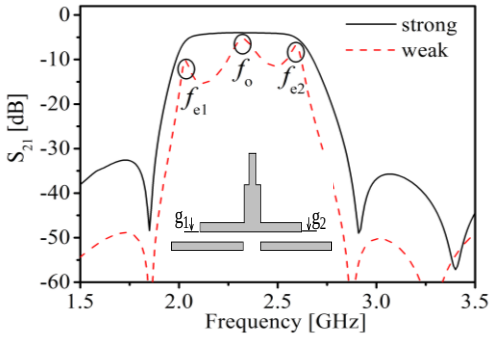

Fig. 3. Response performances under weak and strong coupling schemes.

B. Operating frequency, bandwidth and isolation

Due to the symmetrical topology of proposed FPD, it can be bisected into two identical parts along its symmetrical plane AA' and only half a bisection is considered which is classified into five distinctive sections as illustrated in Fig. 4, so as to simplify our analysis.

According to the power divider's design principle, Port 2 needs to be matched to 50 Ω. Since tuning the coupling lengths of resonator will change the resonance frequency, here the impedance matching is mainly realized by altering Z_r. Figure 5 shows the return loss at Port 2 versus various values of Z_r, including when Z_r=0. Therefore, for a better impedance matching, here we choose Z_r as 65 Ω.

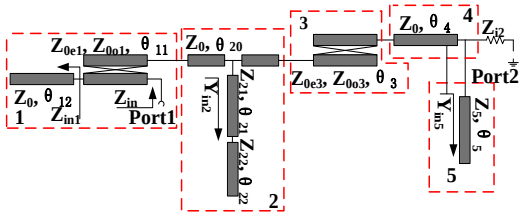

Fig. 4. Half a bisection of equivalent circuit of the proposed FPD in five sections.

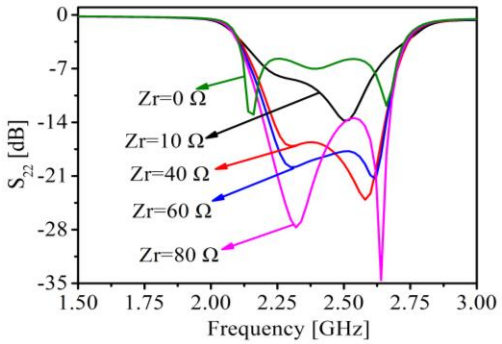

Fig. 5. S_{22} at Port 2 versus various values of Z_r.

Assuming that the electrical lengths of the coupled line section under even- and odd-modes are equal, the transmission matrix of each section can be extracted as:

$$[ABCD_1]=\begin{bmatrix}\dfrac{-d_1(a_1Z_{in1}+b_1)}{a_1e_1Z_{in1}-c_1d_1} & \dfrac{-a_1(a_1Z_{in1}+b_1)}{a_1e_1Z_{in1}-c_1d_1}\\ \dfrac{e_1^{\,2}Z_{in1}-d_1^{\,2}Z_{in1}-a_1d_1}{a_1e_1Z_{in1}-c_1d_1} & \dfrac{-(a_1d_1Z_{in1}+a_1^{\,2}-c_1e_1)}{a_1e_1Z_{in1}-c_1d_1}\end{bmatrix}, \tag{6}$$

$$[ABCD_2]=\begin{bmatrix}\cos\theta_{20} & jZ_0\sin\theta_{20}\\ jY_0\sin\theta_{20} & \cos\theta_{20}\end{bmatrix}\times\begin{bmatrix}1 & 0\\ Y_{in2} & 1\end{bmatrix}\times\begin{bmatrix}\cos\theta_{20} & jZ_0\sin\theta_{20}\\ jY_0\sin\theta_{20} & \cos\theta_{20}\end{bmatrix}, \tag{7}$$

$$[ABCD_3]=\begin{bmatrix}-a_3d_3/c_3e_3 & -a_3^{\,2}/e_3\\ -d_3^{\,2}/e_3+e_3 & -a_3d_3/e_3\end{bmatrix}, \tag{8}$$

$$[ABCD_4]=\begin{bmatrix}\cos\theta_4 & jZ_0\sin\theta_4\\ j\sin\theta_4/Z_0 & \cos\theta_4\end{bmatrix}, \tag{9}$$

$$[ABCD_5]=\begin{bmatrix}1 & 0\\ -jZ_7\cot\theta_7 & 1\end{bmatrix}, \tag{10}$$

where $a_{1/3}=\cos\theta_{11/3}$, $b_1=j(Z_{0e1}+Z_{0o1})\sin\theta_{11/2}$, $c_{1/3}=j(Z_{0e1/3}-Z_{0o1/3})\sin\theta_{11/3}/2$, $d_{1/3}=j(1/Z_{0e1/3}+1/Z_{0o1/3})\sin\theta_{11/3}/2$, $e_{1/3}=j(1/Z_{0e1/3}-1/Z_{0o1/3})\sin\theta_{11/3}/2$, $Z_{in1}=-jZ_0\cot\theta_{12}$, $Y_{in2}=-j(Z_{21}+Z_{22}\cot\theta_{22}\tan\theta_{21})/(Z_{21}(Z_{21}\tan\theta_{21}-Z_{22}\cot\theta_{22}))$.

Then, the transmission matrix of the equivalent circuit in Fig. 4 can be expressed as a multiplication of five matrixes of each section:

$$[ABCD]=[ABCD_1]\times[ABCD_2]\times[ABCD_3]\times[ABCD_4]\times[ABCD_5]. \tag{11}$$

The synthesis method based on the transmission matrix [10] is elucidated to initially determine the operating central frequency and its respective bandwidth. In this context, the input impedance at Port 1 is calculated under the perfect impedance matching at both Port 2 and Port 3:

$$Z_{in}=(Z_{i2}A+B)/(Z_{i2}C+D), \tag{12}$$

where Z_{i2}=50 Ω is the image impedance at Port 2. Subsequently, the reflection and transmission coefficient of Port1 can be elucidated by:

$$S_{11}=(Z_{in}-Z_0)/(Z_{in}+Z_0), \tag{13}$$

$$S_{21}=(0.5-0.5S_{11}^{\,2})^{\frac{1}{2}}. \tag{14}$$

The isolation between Port 2 and 3 can be analyzed through the equivalent circuits under the even-/odd-mode excitations as depicted in Figs. 6 (a) and (b), respectively. When the even-/odd-mode signal is applied to Port 2 and 3, the transmission matrix of the even-/odd-mode equivalent circuit can be derived as:

$$[ABCD_{e/o}]=[ABCD_5]\times[ABCD_4]\times[ABCD_3]\times[ABCD_{2e/o}]\times[ABCD_{1e/o}], \tag{15}$$

where

$$[ABCD_{1e}]=[ABCD_{1o}]=\begin{bmatrix}\dfrac{ce-a^2-adZ_{in1}}{be+aeZ_{in1}} & -a/e\\ \dfrac{e^2Z_{in1}-d^2Z_{in1}-ad}{be+aeZ_{in1}} & -d/e\end{bmatrix}, \tag{16}$$

$$[ABCD_{2o}]=[ABCD_{2e}]\times\begin{bmatrix}1 & 0\\ 2/Z_r & 1\end{bmatrix}=[ABCD_2]\times\begin{bmatrix}1 & 0\\ 2/Z_r & 1\end{bmatrix}. \tag{17}$$

Thus, the input impedance at Port 2 under even-/odd-mode excitation and the transmission coefficient between Port 2 and Port 3 can be elucidated as

$$Z_{ine/o}=\frac{Z_{i1e/o}A_{e/o}+B_{e/o}}{Z_{i1e/o}C_{e/o}+D_{e/o}}, \tag{18}$$

$$S_{23}=Z_0\frac{Z_{ine}-Z_{ino}}{(Z_{ine}+Z_0)(Z_{ino}+Z_0)}, \tag{19}$$

where the image impedance at Port 1 under even-/odd-excitation is 100 Ω and 0 Ω, respectively.

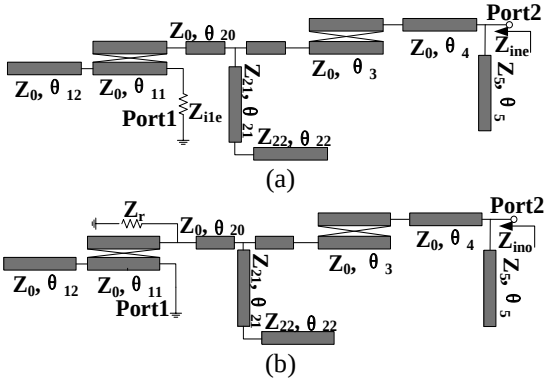

Fig. 6. Equivalent circuit of the proposed FPD under even-/odd-mode excitations: (a) even-mode excitation and (b) odd-mode excitation.

Till now, the analysis method has been described to predict the *S*-matrix of the proposed FPD. Based on this method, a FPD circuit is analyzed and its predicted performance is attained with 3-dB fractional bandwidth of 29.2% at central frequency of 2.18 GHz. As illustrated in Fig. 7, the isolation between Port 2 and 3 is better than 17.0 dB. It should be mentioned that owing to inevasible distinctions caused by the modeling simplification, slight differences are adopted between the geometrical parameters in theoretical analysis and those as denoted in Fig. 1 during circuit design.

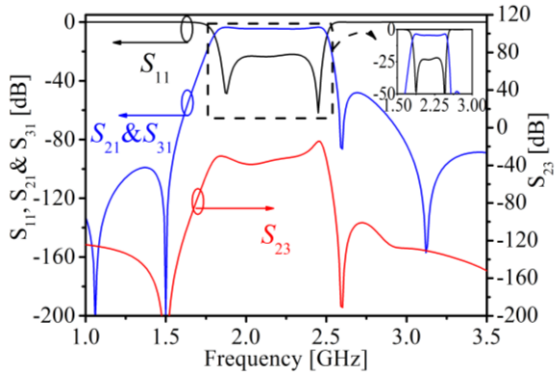

Fig. 7. Calculated results of S-parameters.

III. SIMULATION AND MEASUREMENT RESULTS

For verification, the proposed FPD with an overall size of 0.29 λ_0×0.89 λ_0 has been fabricated on a 0.508 mm thick RO4003C substrate with a dielectric constant of 3.38 and its photograph is shown in the inset of Fig. 8.

The diameter of via hole is 0.6 mm, and the dimensions of proposed FPD are presented in Table 1. Simulation was accomplished by the EM simulator HFSS while the measurement was carried out on the Agilent N5244A network analyzer.

The simulated and measured results are shown in Fig. 8. As can be seen from Fig. 8 (a), the FPD operates from 2.04 GHz to 2.64 GHz with a 3-dB bandwidth of 25.6%. Inside the passband, the measured minimum insertion loss is 0.9 dB with a maximum return loss of 25 dB. Besides, the minimum in-band isolation is 15.5 dB and the out-of-band rejection bandwidth is extended to 7.6 GHz (3.23f_0) with a rejection level of 20 dB. It can be found in Fig. 8 (b) that better than 0.12 dB amplitude imbalance and 0°±3.8° phase difference are both achieved, while at the frequency band of 1.5-2 GHz, the phase imbalance is slightly larger than that at higher frequency but still within the rational range. It should be mentioned that the small discrepancy between measured and simulated results are mainly due to the fabrication tolerance. A comparison between the proposed FPD and other recent designs is tabulated in Table 2. It is seen that the 3-dB bandwidth of this work is wider than those of counterparts in [1], [6] and [9], with an extended isolation bandwidth as well as upper stopband.

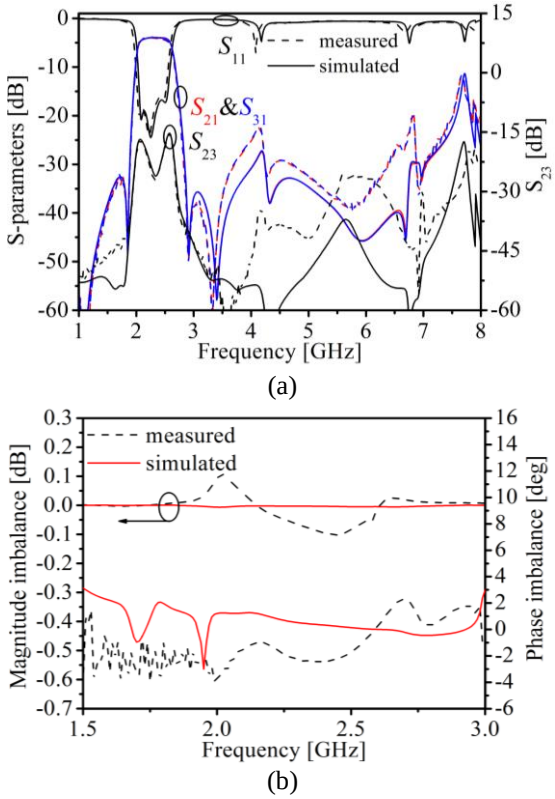

Fig. 8. Measured and simulated results: (a) S11, S21, S31 & S23, and (b) amplitude and phase imbalance.

Table 2: Comparisons among the proposed and previously reported filtering power dividers

	3-dB Bandwidth	Isolation <-15 dB within entire Passband	Harmonic Suppression	Roll Off
[1]	7.1%	No	2.9 f_0	Yes
[6]	3.5%	Yes	Not mentioned	No
[9]	6.5%	Yes	2.6 f_0	Yes
This work	25.6%	Yes	3.23 f_0	Yes

IV. CONCLUSION

In this paper, a new design of compact wideband FPD has been presented. A novel topology is introduced by adding an isolation resistor between two high-impedance stubs of tri-mode resonators for good isolation. Synthesis method and calculative verification have been presented to predict or initially determine its performance. To verify the feasibility of the design concept, a FPD has been then designed, fabricated and measured. Simulated and measured results agree well in the entire design frequency band, which verify the

feasibility of the proposed design method to a great extent. We believe the proposed wideband FPD will be very promising in wireless communication.

REFERENCES

[1] R. Mirzavand, M. Honari, A. Abdipour, and G. Moradi, "Compact microstrip Wilkinson power dividers with harmonic suppression and arbitrary power division ratios," *IEEE Trans. Microw. Theory Tech.*, vol. 61, no. 1, pp. 61-68, Jan. 2013.

[2] K. J. Song, "Compact filtering power divider with high frequency selectivity and wide stopband using embedded dual-mode resonator," *Electron. Lett.*, vol. 51, no. 6, pp. 495-497, Mar. 2015.

[3] S. W. Wong and L. Zhu, "Ultra-wideband power dividers with good isolation and improved sharp roll-off skirt," *IET Microw. Antennas Propag.*, vol. 3, no. 8, pp.1157-1163, Feb. 2009.

[4] B. Zhang and Y. A. Liu, "Wideband filtering power divider with high selectivity," *Electron. Lett.*, vol. 51, no. 23, pp. 1950-1952, Nov. 2015.

[5] J. Y. Shao, S. C. Huang, and Y. H. Pang, "Wilkinson power divider incorporating quasi-elliptic filters for improved out-of-band rejection," *Electron. Lett.*, vol. 59, no. 11, pp. 2848-2855, Nov. 2011.

[6] C. F. Chen and C. Y. Lin, "Compact microstrip filtering power dividers with good in-band isolation performance," *IEEE Microw. Wireless Compon. Lett.*, vol. 24, no. 1, pp. 17-19, Jan. 2014.

[7] S. F. Chao and W. C. Lin, "Filtering power divider with good isolation performance," *Electron. Lett.*, vol. 50, no. 11, pp. 815-817, May 2014.

[8] P. Cheong, K. I. Lai, and K. W. Tam, "Compact Wilkinson power divider with simultaneous bandpass response and harmonic suppression," *IEEE MTT-S International Microwave Symposium Digest*, vol. 23, no. 3, pp. 1588-1591, May 2010.

[9] X. Y. Zhang, K. X. Wang, and B. J. Hu, "Compact filtering power divider with enhanced second-harmonic suppression," *IEEE Microw. Wireless Compon. Lett.*, vol. 23, no. 9, pp. 483-485, Sep. 2013.

[10] D. M. Pozar, *Microwave Engineering*. 3rd ed., New York: Wiley, 2005.

Yijing Deng, received the B.S. degree in Information Countermeasures Engineering from NJUST, Nangjing, China, in 2014. She is currently working toward the Ph.D. degree in Electromagnetic Field and Microwave Technology in NJUST. Her research interest is the design of miniaturized high performance microwave/millimeter-wave passive device and numerical methods in electromagnetics.

Yixuan He is with the Beijing Institute of Technology (BIT), Beijing, China. His research interest is the design of high performance microwave passive components on PCB.

Jianpeng Wang received the M.Sc. and Ph.D. degrees from UESTC, Chengdu, China, in 2004, and 2007, respectively. Since Jan. 2008, he has been with the Ministerial Key Laboratory of JGMT, School of Electronic and Optical Engineering, NJUST. His research interests include the high performance microwave/ millimeter-wave passive components, circuits and systems realized on PCB, LTCC, etc.